

Pyronine B/Graphene Copolymer Modified Carbon Molecular Wire Electrode for Electrochemical Detection of Quercetin

*Xiaoping Zhang, Bo Shao, Lijun Yan, Yaping Lu, Mingxuan Zhao, Xiaoli He, Xuerui Li, Wei Sun**

Key Laboratory of Laser Technology and Optoelectronic Functional Materials of Hainan Province, Key Laboratory of Functional Materials and Photoelectrochemistry of Haikou, College of Chemistry and Chemical Engineering, Hainan Normal University, Haikou 571158, P R China

*E-mail: swyy26@hotmail.com

Received: 24 September 2020 / *Accepted:* 10 November 2020 / *Published:* 30 November 2020

By using cyclic voltammetric method a pyronine B (PB) and graphene (GR) copolymer was electrochemically formed on carbon molecular wire electrode (CMWE) to get the working electrode (named as PB-GR/CMWE). The synergistic functions of PB and GR resulted in the excellent electrochemical performances with higher conductivity and lower interfacial resistances. Voltammetric behaviors of quercetin on PB-GR/CMWE were investigated by cyclic voltammetry, which gave a pair of well-defined redox response in pH 5.0 phosphate buffer solution. Under the selected conditions, the oxidation peak currents were in linear to quercetin concentration from 0.2 ~ 80.0 $\mu\text{mol L}^{-1}$ with the detection limit as $6.37 \times 10^{-8} \text{ mol L}^{-1}$ (3σ). The fabricated PB-GR/CMWE was further used to detect quercetin in compound ginkgo leaf tablets with satisfactory results.

Keyword: Pyronine B; Graphene; Electrochemistry; Quercetin

1. INTRODUCTION

Quercetin is the world's most common flavonoid in plants, which widely exists in various fruits and vegetables, such as tomato, grape, hawthorn and many Chinese herbal medicines. Because of its excellent pharmacological functions including anti-inflammation, anti-viral property, anti-anaphylaxis, anti-oxidant and anti-tumor, quercetin has attracted increasing attentions [1-4]. Various methods have been used for the detection of quercetin so far, including liquid chromatography [5], near-infrared reflectance spectroscopy [6], ultraviolet spectrophotometry [7], chemiluminescence [8], and so on. Although these methods obtain better anti-jamming characteristic and lower detection limit, they are time consuming, cost, and require more complex operations. In recent years electrochemical methods have been noticed due to the advantages such as simple to operate, high performance, and cost-effectivity [9-12]. For instance, Zielinska et al. determined the quercetin in onion bulbs by cyclic

voltammetry [13]. Niu et al. used three-dimensional reduced graphene oxide aerogel modified electrode to study the electrochemical behavior of quercetin [14].

Graphene (GR) has exhibited many novel physicochemical characteristics including thermal and mechanical properties, high carrier mobility and fast electrical conductivity [15,16]. Therefore GR and its related composites have been widely used in electrochemistry and electrochemical sensors [17,18]. Recently, various GR based composites modified electrodes have been prepared with different applications, which exhibit co-contributions of the performances with the properties of single nanomaterial and their synergistic effects [19-22].

Pyronine B (PB) is a kind of organic small molecular dye that often used as a stain of ribonucleic acid [23]. In this article PB and GR were electropolymerized on the carbon molecular wire electrode (CMWE) by electrochemical method to get a PB-GR copolymer modified CMWE. The performance of the PB-GR/CMWE was characterized by electrochemical methods. Moreover, electrochemical behaviors of quercetin on PB-GR/CMWE were fully studied with a sensitive voltammetric method for quercetin analysis further proposed.

2. EXPERIMENTAL

2.1 Instruments and reagents

Cyclic voltammetry and differential pulse voltammetry (DPV) were carried out on a CHI 1210B electrochemical workstation with electrochemical impedance spectroscopy (EIS) on a CHI 750B electrochemical workstation (Shanghai CH Instruments, China). Typical three-electrode system was designed using a PB-GR/CMWE working electrode (apparent area as 0.12 cm^2), a saturated calomel reference electrode (SCE) and a platinum wire counter electrode. Scanning electron microscopic images were conducted with a JSM-6700F scanning electron microscopy (Japan Electron Company, Japan).

Graphite powder (average size $\leq 30 \text{ um}$, Shanghai Colloid Chem. Co., China), diphenylacetylene (DPA, 99%, Aladdin Chem. Co., China) and quercetin (Hongyu Chem. Co., Beijing Institute of Technology) were directly used. Graphene oxide (GO) was synthesized by an improved Hummer method [24, 25]. Phosphate buffer solution (PBS) was used as the supporting electrolyte in the electrochemical procedure. All reagents were of AR grade with doubly distilled water used.

2.2. Electrode fabrication

With the similar procedure as formerly reported [26], CMWE was fabricated by the following procedure. 1.6 g of graphite powder and 0.6857 g of DPA were hand-mixed in an agate mortar to get the mixed carbon paste. After 3 min baking in the drying oven at $75 \text{ }^\circ\text{C}$, the carbon paste was inserted into a glass tube ($\Phi=4 \text{ mm}$) with a copper wire at the opposite end as the electrical conductor. The newly-prepared of CMWE were polished on weighing paper just before use.

The synthesized GO was redispersed in 0.2 mol L⁻¹ PBS and ultrasonicated to get a 1.0 mg mL⁻¹ GO dispersion solution. After 10 min deoxygenation with nitrogen, the GO solution was mixed with 1.0 mol L⁻¹ PB solution with ultrasonication to obtain a PB functionalized GO (PB-GO) mixture solution. Then CMWE was dipped into the PB-GO solution with cyclic voltammetric scan performed in the range of -1.5 V ~ 2.0 V at a scan rate of 80 mV s⁻¹. After 20 cycles, the target electrode (PB-GR/CMWE) was prepared with the surface washed thoroughly by water and dried by a nitrogen blow. Other modified electrodes such as PB/CMWE and GR/CMWE were prepared by similar procedure.

3. RESULTS AND DISCUSSION

3.1. Characteristics of the working electrode

SEM images of CMWE and PB-GR/CMWE were recorded and shown in Fig. 1. Uniformly and smoothly morphology could be observed on CMWE (Fig. 1A), which was owned to the high viscosity of DPA that could fill into the void space of graphite powder with the smoothness of electrode interface improved. When PB and GR were formed homopolymer on CMWE, a foggy structure could be obtained (Fig. 1B). The interface was connected with many small particles on the surface of GR, which indicated that PB and GR were copolymerized to form a hybrid composite with increase of the interfacial roughness.

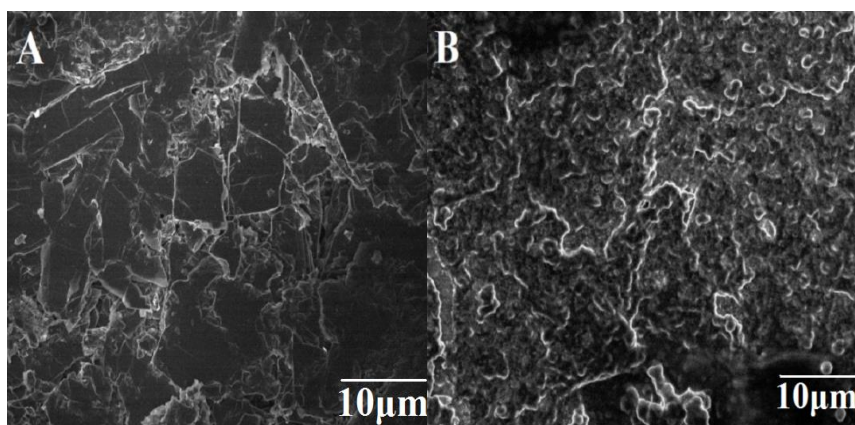


Figure 1. SEM images of CMWE (A) and PB-GR/CMWE (B)

Voltammetric behaviors of various electrodes were obtained in the 1.0 mmol L⁻¹ K₃[Fe(CN)₆] and 0.5 mol L⁻¹ KCl solution with curves shown in Fig. 2A. Compared to the results at CMWE (curve a), the redox peaks currents at PB/CMWE (curve b) and GR/CMWE (curve c) were slightly increased with the peak-to-peak separation (ΔE_p) value decreased, indicating the reversibility of the electrode reaction improved. The redox peaks currents at PB-GR/CMWE were significantly increased (curve d), and a pair of more clearly redox peaks appeared with ΔE_p value further decreased. The result might be due to the high conductivity and the large specific surface area of the organic-inorganic polymer on the surface of CMWE that could expedite the electron transfer and improve interfacial conductivity, implying that this working electrode could present highest catalytic performance.

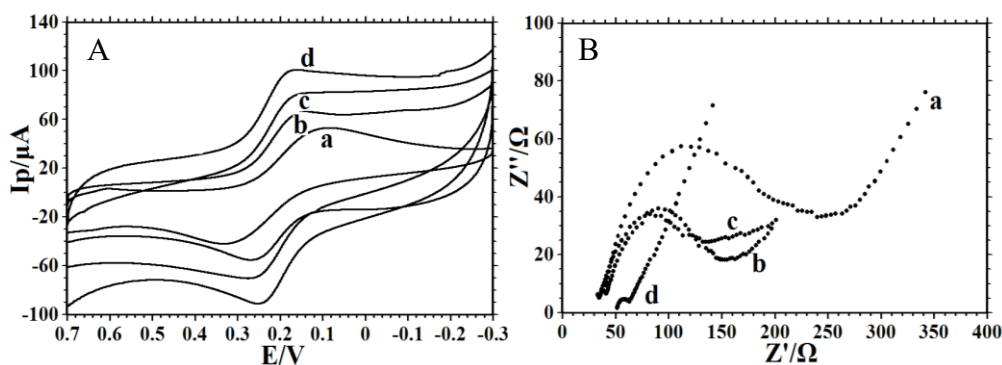


Figure 2. (A): Cyclic voltammograms of different electrodes in a solution of $1.0 \text{ mmol L}^{-1} [\text{Fe}(\text{CN})_6]^{3-}$ and $0.5 \text{ mmol L}^{-1} \text{ KCl}$ at a scan rate of 100 mV s^{-1} . (B): EIS of different electrodes in a solution of $10.0 \text{ mmol L}^{-1} [\text{Fe}(\text{CN})_6]^{3-}$ and $0.1 \text{ mol L}^{-1} \text{ KCl}$ with the frequencies swept from 10^{-1} to 10^5 Hz. Electrodes: (a) CMWE, (b) PB/CMWE, (c) GR/CMWE, (d) PB-GR/CMWE.

These modified electrodes were further studied with EIS analysis to display the impedance of the electrode surface with different modifiers. Nyquist plots of EIS results for different electrodes were shown in Fig. 2 B, which was measured in $10.0 \text{ mmol L}^{-1} [\text{Fe}(\text{CN})_6]^{3-}$ and $0.1 \text{ mol L}^{-1} \text{ KCl}$ solution. It is observed that the value of electron transfer resistance (R_{et}) was 225.36Ω on bare CMWE (curve a), and the R_{et} values were decreased to 128.76Ω and 82.15Ω on PB/CMWE (curve b) and GR/CMWE (curve c), respectively. The smallest R_{et} value was got as 12.17Ω on PB-GR/CMWE (curve d), implying that the synergistic functions of PB-GR copolymer effectively accelerated electron transfer rate and improved electrode conductivity. Then PB-GR/CMWE was utilized as the working electrode to detect quercetin in the following tests.

3.2. Cyclic voltammetric behaviors of quercetin

Fig. 3 shows the cyclic voltammetric behaviors of quercetin ($1.0 \times 10^{-4} \text{ mol L}^{-1}$) at various working electrodes in pH 5.0 PBS. It is observed that a couple of small redox peaks appeared on CMWE (curve a) with the cathodic peak potential of 0.430 V (E_{pc}) and the anodic peak potential of 0.320 V (E_{pa}), and the value of ΔE_p was obtained as 0.110 V . The cathodic and the anodic peak currents were got as $83.47 \mu\text{A}$ (I_{pc}) and $31.15 \mu\text{A}$ (I_{pa}). On PB/CMWE (curve b), E_{pc} and E_{pa} were got as 0.434 V and 0.305 V with I_{pc} and I_{pa} as $69.24 \mu\text{A}$ and $36.68 \mu\text{A}$, respectively. On GR/CMWE (curve c), the values of E_{pc} , E_{pa} , I_{pc} , and I_{pa} were recorded as 0.440 V , 0.313 V , $116.2 \mu\text{A}$, and $54.10 \mu\text{A}$, respectively. It could be concluded that the increased redox peak current was attributed to the electrocatalytic ability of GR film on the electrode surface. While on PB-GR/CMWE (curve d), a pair of well-defined redox peaks were observed with the further increase of the redox peak currents. The E_{pc} and E_{pa} value was 0.432 V and 0.323 V with I_{pc} and I_{pa} value as $137.8 \mu\text{A}$ and $83.43 \mu\text{A}$. The I_{pc} ($1378 \mu\text{A}/1.0 \text{ mmol L}^{-1}$ of quercetin) was almost five-fold larger than that at GR/GCE ($289.2 \mu\text{A}/1.0 \text{ mmol L}^{-1}$ of quercetin) reported in the literature previously [27]. The result indicated that the best responses could be ascribed to the synergistic effects of copolymer that enhanced the electrochemical data of quercetin.

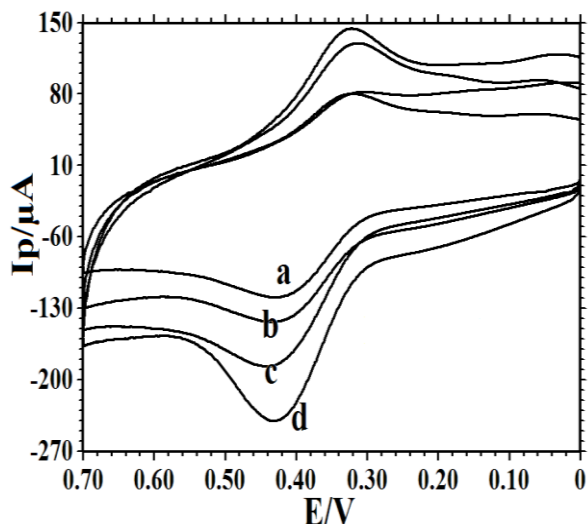


Figure 3. Cyclic voltammograms of 1.0×10^{-4} mol L $^{-1}$ quercetin on (a) CMWE, (b) PB/CMWE, (c) GR/CMWE, (d) PB-GR/CMWE with the scan rate of 100 mV s $^{-1}$.

3.3. Effect of buffer pH

To further investigate the effect of buffer pH on redox responses of quercetin, voltammetric curve of 1.0×10^{-4} mol L $^{-1}$ quercetin on PB-GR/CMWE were obtained. It is worth noting that the peak current experiences an increase and a decrease with the increase of buffer pH. As can be seen in Fig. 4A, the maximum oxidation peak current is acquired at pH 5.0, which was used as the optimal experimental condition. The influence of buffer pH on formal potentials was also investigated, and a good linear relationship was obtained with linear regression equation as $E^{0'}(\text{V}) = -0.0544 \text{ pH} + 0.758$ ($n=8$, $\gamma=0.994$, Fig.4 B). The slope value (-54.4 mV pH^{-1}) was similar with the theoretical value (-59.0 mV pH^{-1}), proving that same number of proton and electron occurred in electrode reaction of quercetin.

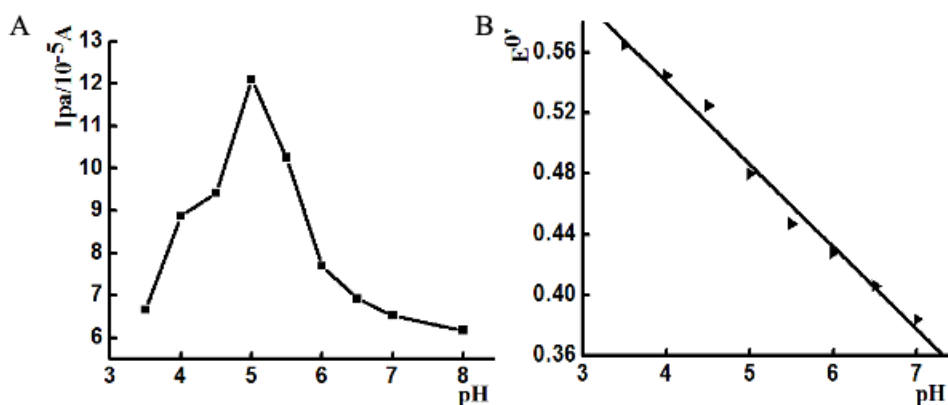


Figure 4. The pH relationship of Ipa (A) and $E^{0'}$ (B) of 1.0×10^{-4} mol L $^{-1}$ quercetin with the scan rate as 100 mVs $^{-1}$.

3.4. Effect of scan rate

Cyclic voltammograms were obtained in the range of 20–500 mVs⁻¹ to investigate the influence of scan rate with curves shown in Fig. 5A. A couple of more clearly redox peaks was obtained at various scan rates and the peak currents increased step by step with scan rate. Fig. 5B showed the relationship between the redox peaks current of quercetin and scan rate with two linear regression equations as $I_{pa}(\mu\text{A}) = -1016.64 v (\text{V/s}) - 20.62$ ($n=14$, $\gamma=0.999$) and $I_{pc}(\mu\text{A}) = 564.99v (\text{V/s}) + 0.26$ ($n=14$, $\gamma=0.999$). The results indicated that the electrode reaction of quercetin on PB-GR/CMWE was an adsorption-controlled process.

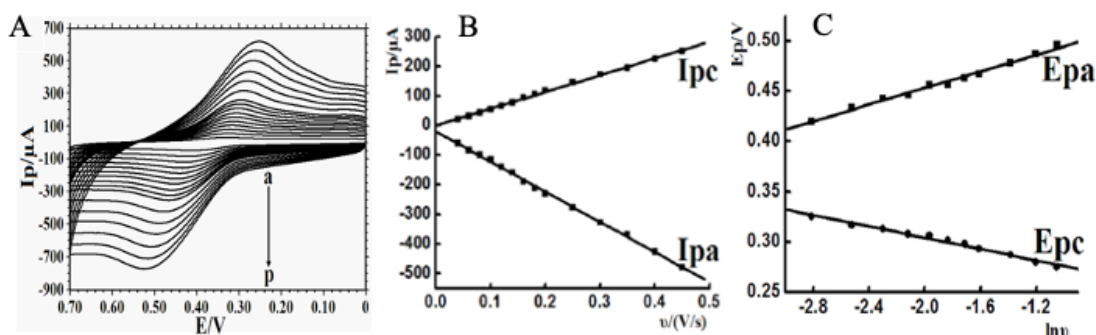


Figure 5. (A) Cyclic voltammograms of 1.0×10^{-4} mol L⁻¹ quercetin on PB-GR/CMWE with various scan rates: (a~p: 0.02, 0.04, 0.06, 0.08, 0.10, 0.12, 0.14, 0.16, 0.18, 0.20, 0.25, 0.30, 0.35, 0.40, 0.45, 0.50 Vs⁻¹); (B) Linear relationship of I_{pa} and I_{pc} versus v ; (C) Linear relationship of E_{pa} and E_{pc} versus $\ln v$.

It is worth noting that the E_{pa} of quercetin continuously increased and the E_{pc} continuously decreased with the increase of scan rate. The relationship of the redox peaks potentials with $\ln v$ were obtained (Fig. 5C) with two linear regression equations as $E_{pa} (\text{V}) = 0.0362 \ln v + 0.536$ ($n=11$, $\gamma=0.995$) and $E_{pc} = -0.0252 \ln v + 0.248$ ($n=11$, $\gamma=0.993$). Based on the following Laviron's equations [28]:

$$E_{pc} = E^{0'} - \frac{RT}{\alpha n F} \ln v \quad (1)$$

$$E_{pa} = E^{0'} + \frac{RT}{(1-\alpha)nF} \ln v \quad (2)$$

$$\log k_s = \alpha \log(1-\alpha) + (1-\alpha) \log \alpha - \log \frac{RT}{nFv} - \frac{(1-\alpha)\alpha n F \Delta E_p}{2.3RT} \quad (3)$$

$$m = \frac{RT}{(1-\alpha)n_\alpha F} \quad m' = \frac{RT}{\alpha n_\alpha F}$$

Where α is charge transfer coefficients, v is scan rate, n refers to the electron transfer number of electrode reaction, k_s refers to electron transfer rate constant, $E^{0'}$ refers to formal potential, F is the Faraday constant. The values of α and n can be calculated as 0.59 and 1.70 by equation (1) and (2), and

the value of k_s was got as 0.27 s^{-1} with the equation (3). The results demonstrate the PB-GR modified electrode provide a fast electron transfer rate for the redox reaction of quercetin.

3.5 Effect of accumulation conditions

Because the electrode reaction was an adsorption-controlled process, effects of accumulation time and potential on electrochemical behavior were further investigated. The biggest current value appeared at potential of 0.5 V when the accumulation potential was changed in the range of $-0.5 \sim 1.0 \text{ V}$, so 0.5 V was selected as the optimal potential condition. When the time was longer than 200 s, the current remained almost stable. The result implied that the absorption equilibrium of quercetin was reached on the electrode surface at 200 s, so we chose the 200 s as the optimal time.

3.6 Calibration curve

DPV of various concentrations quercetin on PB-GR/CMWE was executed in pH 5.0 PBS with curves shown in Fig. 6 A. A good linear relationship of oxidation peak current and quercetin concentration was plotted with linear regression equation as $I_{pa}(\mu\text{A}) = 0.445 C (\mu\text{mol L}^{-1}) + 1.459$ ($n=12$, $\gamma=0.998$) in the range from $0.2 \mu\text{mol L}^{-1}$ to $80.0 \mu\text{mol L}^{-1}$ (Fig. 6 B), and the detection limit was calculated as $6.37 \times 10^{-8} \text{ mol L}^{-1}$ (3σ).

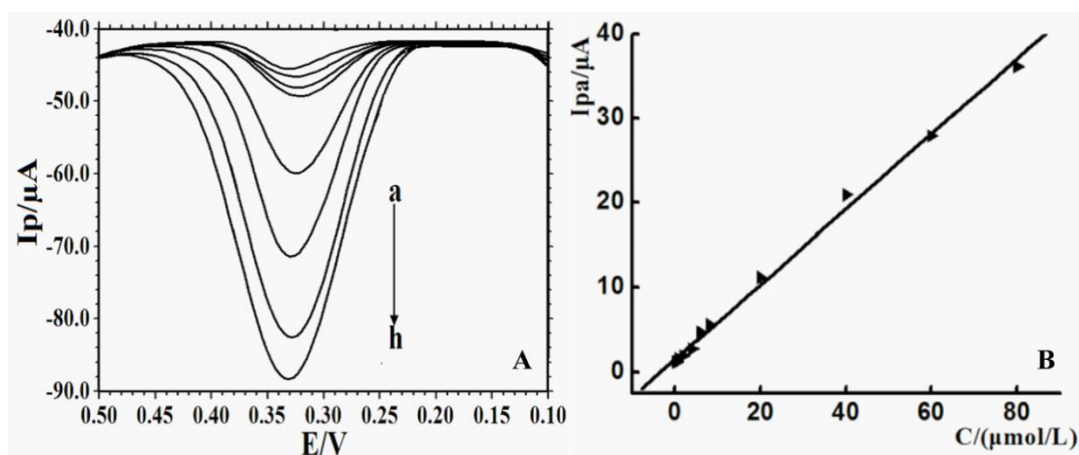


Figure 6. (A) Differential pulse voltammograms of various concentrations quercetin on PB-GR/CMWE (from a to h: 2.0, 4.0, 6.0, 8.0, 20.0, 40.0, 60.0, 80.0 $\mu\text{mol L}^{-1}$). (B) The relationship of the anodic peak current with the quercetin concentration.

Table 1 summarizes the analytical parameters of different detection methods for quercetin analysis. It can be seen that direct electrochemistry detection by PB-GR/CMWE displayed wider detection range and lower detection limit for quercetin analysis, which contributed to better sensitivity for the quercetin detection.

3.7. Interference studies and samples analysis

The influences of some common interfering substances on the detection of 1.0×10^{-4} mol L⁻¹ quercetin using the modified electrode was investigated in pH 5.0 PBS, and the results were listed in Table 2. It is seen that these interfering substances did not disturb the determination, therefore PB-GR/CMWE exhibited good selectivity for quercetin analysis without the interference of commonly coexisting substances.

Table 1. Comparison of different methods for quercetin determination

methods	Liner range (mol L ⁻¹)	Detection limit (mol L ⁻¹)	References
Spectroscopy	$3.3 \times 10^{-6} \sim 4.0 \times 10^{-5}$	2.5×10^{-6}	[29]
High performance liquid chromatography	$6.3 \times 10^{-5} \sim 9.3 \times 10^{-4}$	9.6×10^{-6}	[30]
Capillary electrophoresis	$1.3 \times 10^{-6} \sim 3.3 \times 10^{-4}$	3.3×10^{-7}	[31]
Capillary zone electrophoresis	$1.7 \times 10^{-6} \sim 4.0 \times 10^{-5}$	9.0×10^{-7}	[32]
voltammetry with PB-GR/CMWE	$2.0 \times 10^{-7} \sim 8.0 \times 10^{-5}$	6.37×10^{-8}	This work

Table 2. Influence of coexisting substances on the determination of 1.0×10^{-4} mol L⁻¹ quercetin (n=3)

Coexisting substance	Concentration	Relative error (%)
Glucose	20.0 mg L ⁻¹	-0.38
Uric acid	20.0 mg L ⁻¹	-0.68
Ascorbic acid	20.0 mg L ⁻¹	0.45
Vitamin C	20.0 mg L ⁻¹	2.17
L-cysteine	20.0 mg L ⁻¹	0.59
Dopamine	20.0 mg L ⁻¹	2.16
Resorcinol	20.0 mg L ⁻¹	-1.38
Mg ²⁺	4.0×10^{-5} mol L ⁻¹	-1.15
Zn ²⁺	4.0×10^{-5} mol L ⁻¹	-2.47
K ⁺	1.0×10^{-2} mol L ⁻¹	0.52
Ca ²⁺	4.0×10^{-5} mol L ⁻¹	0.33
Al ³⁺	4.0×10^{-5} mol L ⁻¹	3.01
Na ⁺	1.0×10^{-2} mol L ⁻¹	2.71
Cu ²⁺	4.0×10^{-5} mol L ⁻¹	1.65
Fe ²⁺	4.0×10^{-5} mol L ⁻¹	-0.97

The PB-GR/CMWE was further applied to the detection of quercetin content in ginkgo leaf tablets, which were purchased from Shanghai Xinyi Bailuda Pharmaceutical Ltd. Co. (1215710H) and Zhejiang Conba Pharmaceutical Ltd. Co. (12157127) with the labelled amount as 19.2 mg per tablet. The tablet was firstly weighed and crushed in an agate mortar for 20 min to get the powder, which was dissolved in alcohol to make a 10 mL solution and analyzed by the proposed procedure. To further investigate the recovery, standard addition method was used with the addition of quercetin standard solution and the results were shown in Table 3. All the recovery value was in the range from 95.40% to 98.10%, proving the practical applications.

Table 3. Analysis of quercetin content in ginkgo leaf tablets (n=6)

Drug samples	Labelled ($\mu\text{mol L}^{-1}$)	Found ($\mu\text{mol L}^{-1}$)	Added ($\mu\text{mol L}^{-1}$)	Detected ($\mu\text{mol L}^{-1}$)	Recovery (%)	RSD (%)
1215710H	30.10	28.91	10.00	39.64	95.40	1.03
12157127	30.10	29.04	10.00	39.91	98.10	1.96

3.8. Stability and reproducibility

To further investigate the stability and reproducibility of PB-GR/CMWE, we tested the modified electrode that was stored 2 weeks at room temperature, and the initial current response of the modified electrode was remained constant. The same PB-GR/CMWE was used for ten parallel analysis of 1.0×10^{-4} mol L⁻¹ quercetin and relative standard deviation (RSD) value was calculated as 2.04%, indicating the modified electrode exhibited good reproducibility. Six PB-GR/CMWEs were prepared and used in 1.0×10^{-4} mol L⁻¹ quercetin solution, and the RSD value was calculated as 1.63%. Therefore PB-GR/CMWE showed good stability and reproducibility for routine application.

4. CONCLUSIONS

In this article a PB-GR copolymer modified CMWE was obtained by electrochemical copolymerization. Electrochemical response of quercetin on PB-GR/CMWE was investigated by CV with the value of α , n and k_s calculated as 0.59, 1.7 and 0.27 s^{-1} . The results showed the PB-GR modified electrode could generate a fast electron transfer rate for redox reaction of quercetin. Under the selected conditions, a good linearity was established between the DPV oxidation peak current and the quercetin concentration in the range from $0.2 \mu\text{mol L}^{-1}$ to $80.0 \mu\text{mol L}^{-1}$ with a detection limit of 6.37×10^{-8} mol L⁻¹ (3σ). For the quercetin detection, the prepared PB-GR/CMWE showed the advantages of wider linear range and lower detection limit, which proved that GR and PB copolymer modified electrode had splendid analytical applications in the electrochemical sensor.

ACKNOWLEDGMENTS

This project was supported by the Hainan Provincial Natural Science Foundation of China (2018CXTD336), the National Natural Science Foundation of China (61864002), Open Foundation of

Key Laboratory of Laser Technology and Optoelectronic Functional Materials of Hainan Province (2020LTOM02).

References

1. Z. F. Cai, H. Y. Li, J. L. Wu, L. Zhu, X. R. Ma and C. F. Zhang, *RSC Adv.*, 10 (2020) 8989.
2. J. A. Ross and C. M. Kasum, *Annu. Rev.*, 22 (2002) 19.
3. S. Asma, S. Tayebbeh and M. Ali, *Electroanal.*, 32 (2020) 581.
4. D. F. Birt, S. Hendrich and W. Q. Wang, *Pharmacol. Therapeut.*, 90 (2001) 157.
5. Y. Wang, J. Cao, J. H. Weng and S. Zeng, *J. Pharm. Biomed. Anal.*, 39 (2005) 328.
6. X. H. Zhou and B. R. Xiang, *J. Sep. Sci.*, 40 (2007) 338.
7. S. J. Patil and V. R. Salunkhe, *Inter. J. Res. Ayurveda Pharm.*, 3 (2012) 267.
8. J. B. He, X. Q. Lin and J. Pan, *Electroanal.*, 17 (2005) 1681.
9. X. L. Niu, Z. R. Wen, X. B. Li, W. S. Zhao, X. Y. Li, Y. Q. Huang, Q. T. Li, G. J. Li and W. Sun, *Sens. Actuators B. Chem.*, 255 (2018) 471.
10. E. Demir, A. Senocak, M. Tassebedo-Koubangoye, E. Demibas and H. Y. Aboul-Enein, *Curr. Anal. Chem.*, 16 (2020) 176.
11. W. Sun, X. Z. Wang, H. H. Zhu, X. H. Sun, F. Shi, G. N. Li and Z. F. Sun, *Sens. Actuators B. Chem.*, 178 (2013) 443.
12. W. Sun, Y. H. Wang, Y. G. Lu, A. H. Hu, F. Shi and Z. F. Sun, *Sens. Actuators B. Chem.*, 188 (2013) 564.
13. D. Zielińska, L. Nagels and M.K. Piskula, *Anal. Chim. Acta*, 617 (2008) 22.
14. X. L. Niu, X. Y. Li, W. Chen, X. B. Li, W. J. Weng, C. X. Yin, R. X. Dong, W. Sun and G. J. Li, *Mater. Sci. Eng. C.*, 89 (2018) 230.
15. K. K. Niu, P. Li, Z. X. Huang, L. J. Jiang and H. Bagci, *IEEE J. Multiscale Multiphys. Comput. Tech.*, 5 (2020) 44.
16. A. Nimbalkar and H. Kim, *Nano. Micro. Lett.*, 12 (2020) 1.
17. W. Chen, X. Niu, X. Li, X. Li, G. Li, B. He, Q. Li, W. Sun, *Mater. Sci. Eng. C*, 80 (2017) 135.
18. G. Ran, Y. Li and Y. Xia, *Monatsh. Chem.*, 151 (2020) 293.
19. L. N. Jin, P. Liu, C. Jin, J. N. Zhang and S. W. Bian, *J. Colloid Interface Sci.*, 510 (2018) 1.
20. S. Z. Mohammadi, H. Beitollahi and N. M. Rahimi, *J. Anal. Chem.*, 74 (2019) 345.
21. W. Sun, Y. H. Wang, Y. Y. Zhang, X. M. Ju, G. G. Li and Z. F. Sun, *Anal. Chim. Acta*, 751 (2012) 59.
22. W. Sun, L. L. Cao, Y. Deng, S. X. Gong, F. Shi, G. N. Li and Z. F. Sun, *Anal. Chim. Acta*, 781 (2013) 41.
23. F. Gao, Y. X. Li, L. Zhang and L. Wang, *Spectrochim. Acta A*, 60 (2004) 2505.
24. S. J. Park and R. S. Ruoff, *Nat. Nanotechnol.*, 4 (2009) 217.
25. T. Szabó, A. Szeri and I. Dékány, *Carbon*, 43 (2005) 87.
26. W. Sun, L. Xu, T. T. Li, X. Z. Wang, G. J. Li and Z. F. Sun, *J. Chin. Chem. Soc.*, 59 (2012) 1571.
27. M. Arvand and M. Anvari, *J. Iran. Chem. Soc.*, 10(2013)841.
28. R.S. Nicholson and I. Shain, *Anal. Chem.*, 36 (1964) 706.
29. X. N. Lu, C. F. Ross, J. R. Powers and B. A. Rasco, *J. Agr. Food Chem.*, 59 (2011) 6376.
30. R. Bugianesi, M. Serafini, F. Simone, D. Y. Wu, S. Meydani, A. Ferro-Luzzi and G. Maiani, *Anal. Biochem.*, 284 (2000) 296.
31. H. T. Duan, Y. Chen and G. Chen. *J. Chromatogr. A*, 1217 (2010) 4511.
32. G. Chen, H. Zhang and J. Ye, *Anal. Chim. Acta*, 423 (2000) 69.